

Articles

Table of Contents

Circulation. 1996;94:407-424

doi: 10.1161/01.CIR.94.3.407

(Circulation. 1996;94:407-424.)

© 1996 American Heart Association, Inc.

Articles

Role of the Tricuspid Annulus and the Eustachian Valve/Ridge on Atrial Flutter

Relevance to Catheter Ablation of the Septal Isthmus and a New Technique for Rapid Identification of Ablation Success

Hiroshi Nakagawa, MD, PhD; Ralph Lazzara, MD; Terrance Khastgir, MD; Karen J. Beckman, MD; James H. McClelland, MD; Shinobu Imai, MD; Jan V. Pitha, MD, PhD; Anton E. Becker, MD; Mauricio Arruda, MD; Mario D. Gonzalez, MD; Lawrence E. Widman, MD, PhD; Michael Rome, MD; Jeffrey Neuhauser, MD; Xunzhang Wang, MD; James D. Calame, RN; Maurice D. Goudeau, RN; Warren M. Jackman, MD

the Department of Medicine, University of Oklahoma Health Sciences Center, and the Department of Veterans Affairs Medical Center, Oklahoma City, Okla, and Academic Medical Center (A.E.B.), Amsterdam, Netherlands. Presented in part at the 14th Annual Scientific Sessions of the North American Society of Pacing and Electrophysiology, May 1993, San Diego, Calif.

Correspondence to Warren M. Jackman, MD, Department of Medicine/Cardiovascular Section, University of Oklahoma Health Sciences Center, 920 SL Young Blvd, Room 5SP300, Oklahoma City, OK 73104.

Abstract

Background Typical atrial flutter (AFL) results from right atrial reentry by propagation through an isthmus between the inferior vena cava (IVC) and tricuspid annulus (TA). We postulated that the eustachian valve and ridge (EVR) forms a line of conduction block between the IVC and coronary sinus (CS) ostium and forms a second isthmus (septal isthmus) between the TA and CS ostium.

Methods and Results Endocardial mapping in 30 patients with AFL demonstrated atrial activation around the TA in the counterclockwise direction (left anterior oblique projection). Double atrial potentials were recorded along the EVR in all patients during AFL. Pacing either side of the EVR during sinus rhythm also produced double potentials, which indicated fixed anatomic block across EVR. Entrainment pacing at the septal isthmus and multiple sites around the TA produced a Δ return interval ≤ 8 ms in 14 of 15 patients tested. Catheter ablation eliminated AFL in all patients by ablation of the septal isthmus in 26 patients and the posterior isthmus in 4. AFL recurred in 2 of 12 patients (mean follow-up, 33.9 ± 16.3 months) in whom ablation success was defined by the inability to reinduce AFL, compared with none of 18 patients (mean follow-up, 10.3 ± 8.3 months) in whom success required formation of a complete line of conduction block between the TA and the EVR, identified by CS pacing that produced atrial activation around the TA only in the counterclockwise direction and by pacing the posterior TA with only clockwise atrial activation.

Conclusions (1) The EVR forms a line of fixed conduction block between the IVC and the CS; (2) the EVR and the TA provide boundaries for the AFL reentrant circuit; and (3) verification of a complete line of block between the TA and the EVR is a more reliable criterion for long-term ablation success.

Key Words: atrial flutter • mapping • catheter ablation • radiofrequency

Introduction

Atrial flutter was described early in this century¹ and was considered to be the result of a macroreentrant circuit in the right atrium in the vicinity of the venae cavae.² In recent decades, this hypothesis was supported by mapping of activation in animal models of atrial flutter and typical atrial flutter in humans with sequential catheter recordings and with simultaneous multielectrode maps of atrial activation during surgery.^{4 5 6 7 8 9 10 11 12 13 14 15 16 17 18} The prevalent interpretation of the activation maps has been that the reentrant circuit contains a long segment that propagates anteriorly in the interatrial septum and another that propagates posteriorly along the lateral wall of the right atrium, but the specific course of the circuit in its anterior and posterior aspects has been unclear. A line of conduction block extending between the venae cavae has been thought to separate the septal and free wall segments.^{19 20} In recent years, it has been shown that the reentrant circuit courses between the inferior vena cava and the tricuspid annulus posteriorly and that this posterior isthmus is an opportune site to interrupt the circuit with a lesion induced by radiofrequency current.^{21 22 23}

We recently postulated the presence of a second line of conduction block extending between the inferior vena cava and the coronary sinus ostium that forces the reentrant impulse to propagate between the coronary sinus ostium and the tricuspid annulus and forms another, more narrow isthmus (septal isthmus) amenable to ablation.^{24 25} In this hypothesis, the reentrant atrial wavefront propagates around the tricuspid annulus, between the annulus and the inferior vena cava posteriorly (site A in Fig 1 \blacklozenge), and arrives at the line of block between the coronary sinus ostium and the inferior vena cava (site B in Fig 1 \blacklozenge). The impulse travels anteriorly only through the region between the coronary sinus ostium and the tricuspid annulus (site C in Fig 1 \blacklozenge). Atrial activation then proceeds anteriorly along the tricuspid annulus (site D in Fig 1 \blacklozenge) and simultaneously pivots around the coronary sinus ostium, back toward the inferior vena cava (site E in Fig 1 \blacklozenge). Electrograms in the region of the line of block would be expected to exhibit two distinct atrial potentials separated by an isoelectric interval (double potentials).^{19 20 24 25 26 27 28 29} The first potential is generated by the arriving wavefront on the posterior side of the line of block (site B in Fig 1 \blacklozenge), whereas the second potential is generated by the

returning atrial wavefront on the anterior side of the line of the block (site E in Fig 1 \blacklozenge). Electrodes positioned on the proximal (posterior) side of the block would exhibit a larger, sharper first potential and a smaller, rounded (distant-appearing) second potential, whereas electrodes positioned on the distal (anterior) side of the block would record a small first potential and a larger second potential.^{27 29}

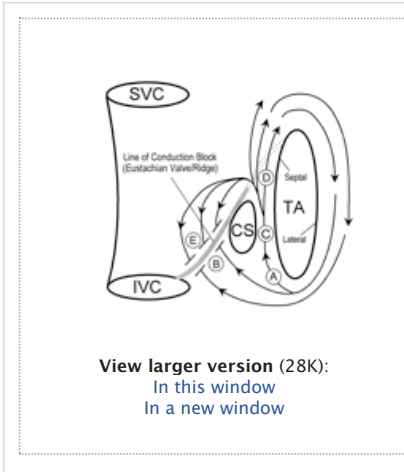


Figure 1. Schematic of the right atrium, as viewed in the right anterior oblique projection, illustrates the hypothesized reentrant circuit in typical atrial flutter (arrows) and the role of the eustachian valve and ridge in forming a line of conduction block between the inferior vena cava (IVC) and the coronary sinus ostium (CS). The eustachian valve/ridge and the tricuspid annulus (TA) form boundaries of a protected channel within the reentrant circuit, beginning with the posterior isthmus (between the TA and the IVC, site A) and ending with the septal isthmus (between the TA and the CS, site C). Dashed lines represent the anterior end of the tendon of Todaro, which has overlying right atrial myocardium. SVC indicates superior vena cava.

Entrainment pacing also can be used to verify the line of block. Entrainment pacing (at a cycle length slightly shorter than the flutter cycle length) from a site within the reentrant circuit would produce an identical P (flutter) wave and atrial activation sequence except for a small area of antidromic activation close to the pacing site.^{5 30 31 32 33 34} The interval from the last pacing stimulus to the return atrial potential recorded at the pacing site would be very close (within 10 ms) to the atrial flutter cycle length.^{30 31 32 33 34} The response to entrainment pacing at the atrial myocardium below the line of block (identified by double potentials with a larger first potential, site B in Fig 1 \blacklozenge) would be similar to that described for a "blind alley" connecting to the reentrant circuit in ventricular tachycardia.^{31 32 33 34} The atrial activation sequence during pacing would be identical to the flutter activation sequence (concealed entrainment), but the interval from the last pacing stimulus to the return atrial potential would be significantly longer than the flutter cycle length. If there were no line of block, the interval between the last pacing stimulus and the return atrial potential would be approximately equal to the flutter cycle length.

The purpose of this study was to test the hypothesis that, in typical atrial flutter, a line of conduction block exists between the coronary sinus ostium and the inferior vena cava that forces the reentrant impulse through a relatively narrow "septal isthmus" between the coronary sinus ostium and the tricuspid annulus. The probable anatomic location for this line of block would be the eustachian valve and ridge (Fig 2A \blacklozenge). We tested this hypothesis using (1) intracardiac mapping (to identify double potentials), (2) entrainment pacing (concealed entrainment with a return interval longer than atrial flutter cycle length after pacing below the eustachian valve/ridge), and (3) radiofrequency catheter ablation of the septal isthmus to determine whether this produces complete posterior-anterior conduction block for atrial wavefronts that propagate septally between the inferior vena cava and the tricuspid annulus and eliminates atrial flutter.



Figure 2. Photographs of the right atrial septum taken in the right anterior oblique projection in two autopsy hearts to illustrate the anatomic relationship of the eustachian valve (EV) and eustachian ridge (ER) to the inferior vena cava (IVC), coronary sinus ostium (CS), and thebesian valve (ThV) in A and D. Note the continuity between the EV and the ThV in D, which might produce a continuous line of conduction block, compared with the more muscular region between the ER and the CS in A, which might allow conduction between the ER and the CS. B shows the location of the orthogonal electrode catheter extending along the EV and ER, between the IVC and the CS. C illustrates the lines of ablation across the septal isthmus (SI) and the posterior isthmus (PI). Note the shorter length and smoother surface across the SI than the PI. FO indicates fossa ovalis; TA, tricuspid annulus.

Methods

Study Population

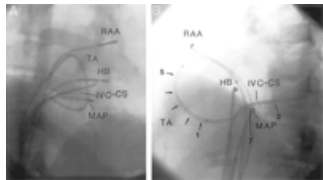
The study population consisted of 30 patients referred for catheter ablation of atrial flutter (Table 1 \blacklozenge). There were 19 men and 11 women, ranging in age from 20 to 75 years (mean, 50 \pm 16 years). Atrial flutter with typical flutter wave morphology (inverted sawtooth pattern in the inferior ECG leads) was the predominant clinical arrhythmia. Atrial flutter was chronic/incessant in 11 patients and paroxysmal in 19 of the 30 patients (63%). At least one episode of atrial fibrillation had been documented in 12 of the 30 patients (40%) and episodes of atrial tachycardia in 2 patients. A mean of 3.5 \pm 1.4 (range, 2 to 6) antiarrhythmic drugs had failed to prevent recurrences of the atrial flutter. Palpitations and other symptoms that had been attributed to atrial flutter were present for a mean of 7 \pm 6.3 years. Atrial flutter produced syncope or presyncope in 13 patients. Structural heart disease was present in 23 of the 30 (77%) patients. Echocardiographic evidence of left atrial enlargement (>4 cm) and/or right atrial enlargement was present in 15 of the 30 (50%) patients. Seven of the 30 (23%) patients had previously undergone an unsuccessful attempt at catheter ablation of the atrial flutter at another institution. One of these patients (No. 7) underwent an atrioventricular nodal modification procedure (using the anterior approach) after failure to eliminate the atrial flutter.

Table 1. Patient Characteristics

[View this table:](#)
[In this window](#)
[In a new window](#)

Electrophysiological Study Protocol

Classes I and III antiarrhythmic drugs were withdrawn at least 5 days before study and aspirin (325 mg daily) was administered 1 day before the study. After providing written informed consent, each patient underwent electrophysiological study in the fasting state under heavy sedation with fentanyl (25 to 100 µg/h) and midazolam (1 to 4 mg/h). Oxygen saturation was monitored with a pulse oximeter, and expired carbon dioxide was monitored with a capnometer. Five multipolar electrode catheters (2-mm interelectrode spacing or orthogonal electrodes) were inserted percutaneously into the right subclavian vein and the right and left femoral veins. Three of the catheters were advanced to the right atrial appendage, His bundle region, and coronary sinus. A 7F deflectable catheter with 20 electrodes spaced in 2-7-2-mm intervals (Halo catheter, Cordis Webster) was positioned around the tricuspid annulus to record atrial activation close to the lateral and posterior tricuspid annulus (TA in Fig 3♦). The remaining catheter was used for right atrial mapping (MAP in Fig 3♦). One of these catheters (or an additional catheter) was positioned in the right ventricle during the ablation portion of the procedure.



[View larger version \(89K\):](#)
[In this window](#)
[In a new window](#)

Figure 3. Radiographs in the right anterior oblique projection (A) and left anterior oblique projection (B) show the positions of the multielectrode catheters in the right atrial appendage (RAA), His bundle region (HB), around the tricuspid annulus (TA), along the eustachian valve/ridge between the inferior vena cava and the coronary sinus (IVC-CS), and the mapping catheter (MAP) positioned at the septal isthmus. Arrows around the TA catheter identify the locations of bipolar electrode pairs. Electrograms are shown in Figs 10 and 11♦♦.

In 18 of the 30 patients, the orthogonal coronary sinus catheter was advanced from the inferior vena cava to the proximal coronary sinus to obtain recordings along the eustachian valve/ridge between the inferior vena cava and the coronary sinus ostium (Fig 2B♦ and IVC-CS in Fig 3♦). A 7F deflectable catheter was used, which had 8 orthogonal electrode pairs with 1.5-mm spacing between orthogonal pairs (Cordis Webster). The shaft of this catheter extends 2 cm beyond the distal orthogonal electrode to anchor the catheter in the coronary sinus. In the remaining patients, electrograms from the region of the eustachian valve/ridge were obtained with the right atrial mapping catheter.

Close bipolar intracardiac electrograms (2-mm spacing or orthogonal electrodes) were recorded from each catheter with a filter bandwidth of 30 to 500 Hz and were displayed at low gain (5 to 20 mV/cm).

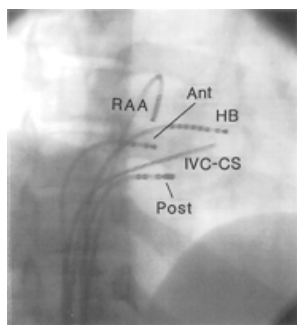
In patients with sinus rhythm at the onset of the procedure, atrial flutter was induced by programmed atrial stimulation with up to three extrastimuli and burst pacing at two atrial sites (right atrial appendage and posterior or posterolateral coronary sinus). If atrial flutter was not induced or was not sustained in the baseline state, isoproterenol (0.5 to 2 µg/min) was administered by continuous infusion and programmed atrial stimulation was repeated.

During atrial flutter, mapping of the right atrium and coronary sinus was performed to identify the atrial activation sequence along the tricuspid annulus, around the coronary sinus ostium, along the region between the coronary sinus ostium and the inferior vena cava (including the eustachian valve/ridge), and in the proximal coronary sinus. Entrainment pacing was performed in 15 of the 30 patients at (1) the posteroseptal right atrium between the coronary sinus ostium and the tricuspid annulus (site C in Fig 1♦), (2) anterior and posterior to the line of double potentials extending along the eustachian valve/ridge between the coronary sinus ostium and the inferior vena cava (sites E and B in Fig 1♦), and (3) at several free wall sites around the tricuspid annulus. Entrainment pacing was performed during atrial flutter at a cycle length 15 to 25 ms shorter than the flutter cycle length. The sequence of atrial activation at all electrode recording sites during entrainment pacing was compared with the atrial activation sequence at these same sites during atrial flutter. The return interval was defined as the interval from the last pacing stimulus to the return atrial potential, which was recorded at the pacing site. When amplifier saturation prevented the recording of the return atrial potential at the pacing site, the timing of the return atrial potential was estimated from the timing of return atrial potentials recorded close to the pacing site. The Δ return interval was defined as (return interval) minus (flutter cycle length). The Δ return interval was used as an estimation of the distance of the entrainment pacing site from the reentrant circuit.

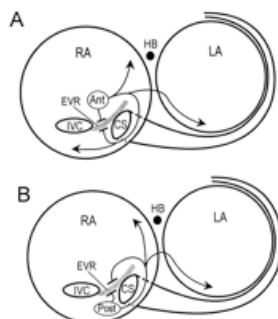
In 15 of the 19 patients who were in sinus rhythm before ablation, atrial pacing (at long cycle lengths) was used to determine whether the line of conduction block along the eustachian valve/ridge was present in the absence of atrial flutter (fixed anatomic block versus functional block during atrial flutter). Two deflectable electrode catheters were positioned just anterior and posterior to the eustachian valve/ridge (Fig 4♦). Atrial pacing (cycle length >500 ms) was performed individually from the anterior and posterior catheters, and the timing of atrial activation at the opposite catheter was compared with the timing of atrial activation at the coronary sinus ostium. Later atrial activation at the opposite catheter than at the coronary sinus ostium (or the region between the tricuspid annulus and the coronary sinus ostium) would suggest the presence of fixed anatomic conduction block at the eustachian valve/ridge with propagation of the paced atrial wavefront around the coronary sinus ostium or around the anterior portion of the eustachian ridge (Fig 5♦). Earlier atrial activation at the catheter opposite to that at the coronary sinus ostium would indicate the presence of conduction across the eustachian valve/ridge and suggest that the block along the eustachian valve/ridge during atrial flutter is functional.

Figure 4. Radiograph in the right anterior oblique projection shows the two electrode catheters used for atrial pacing on the anterior (Ant) and posterior (Post) sides of the eustachian valve/ridge, which lies parallel to the IVC-CS catheter. The electrograms are shown in Fig 13♦. Same patient as in Figs 3, 10, and 11♦♦

♣. Abbreviations as in Fig 3♣.



View larger version (146K):
[In this window](#)
[In a new window](#)



View larger version (31K):
[In this window](#)
[In a new window](#)

Figure 5. Schematics of the right atrium (RA) and left atrium (LA) as viewed in the left anterior oblique projection illustrate the expected pattern of atrial activation in the presence of a line of conduction block along the eustachian valve/ridge (EVR) during atrial pacing anterior to the EVR in A and posterior to the EVR in B. Ant indicates anterior pacing site; Post, posterior pacing site; and HB, His bundle. Other abbreviations as in Fig 3♣.

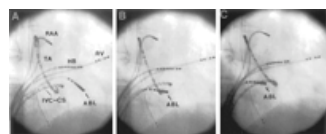
Catheter Ablation

The primary approach for radiofrequency catheter ablation of the atrial flutter was to create a line of atrial conduction block between the tricuspid annulus and the coronary sinus ostium (Line SI in Fig 2C♣, Fig 6A♣, and Fig 7A and 7B♣♣). If the eustachian valve/ridge provides a line of block between the coronary sinus ostium and inferior vena cava, that ablation should create an arc of conduction block (tricuspid annulus–coronary sinus ostium–inferior vena cava) and eliminate the atrial flutter (Fig 6A♣).



View larger version (16K):
[In this window](#)
[In a new window](#)

Figure 6. Schematics of the right atrium in the right anterior oblique projection illustrate the three approaches used in this study for ablation of typical atrial flutter. A, Contiguous ablation line (wide gray line) across the septal isthmus from the TA (at the level of the posterior margin of the CS ostium) to the posteroapical margin of the CS ostium (approach A). In patients without atrial conduction between the CS ostium and the eustachian ridge, this ablation line should produce a complete arc of conduction block from the TA to the CS ostium and to the IVC and eliminate typical and reverse typical atrial flutter. B, Extension of the ablation line, produced by approach A, along the posterior margin of the CS ostium and to the eustachian ridge (approach A and B). Dashed arrow represents atrial conduction between the CS ostium and the eustachian ridge. Approach A and B corresponds to the SI ablation line in Fig 2C♣. C, Contiguous ablation line across the posterior isthmus from the TA to the IVC or the EVR (approach C). This corresponds to the PI ablation line in Fig 2C♣. Abbreviations as in previous figures.



View larger version (74K):
[In this window](#)
[In a new window](#)

Figure 7. Radiographs in the right anterior oblique projection show the ablation catheter (ABL) positions during ablation along the septal isthmus, beginning at the tricuspid annulus at the level of the posterior margin of the coronary sinus ostium (A) and extending to the posteroapical margin of the coronary sinus ostium (B), completing ablation approach A. Extension of the ablation line to the eustachian ridge (C) completes ablation approach A and B. RV indicates right ventricle; other abbreviations as in previous figures.

The ablation catheter was inserted through one of the right femoral venous sheaths, and the tip electrode was positioned against the posteroseptal right atrium, close to the tricuspid annulus at the level of the posterior margin of the coronary sinus ostium. During atrial flutter, the distal bipolar electrogram at this site recorded a single atrial potential that was closer in timing to the first potential of the double potentials recorded just behind the coronary sinus ostium. This electrogram pattern was thought to represent activation in the proximal portion of the septal isthmus between the tricuspid annulus and the coronary sinus ostium. Sites that recorded atrial activation closer in timing to the second potential of the double potentials were avoided because this activation pattern could represent activation at a site distal to the exit of the septal isthmus. The tip electrode was then advanced slightly toward the right ventricle (at the level of the posterior margin of the coronary sinus

ostium) until the distal bipolar electrogram recorded a low-amplitude atrial potential with a large, sharp ventricular potential, indicating a location close to the tricuspid annulus (Fig 7A \blacklozenge). Radiofrequency current (550 to 650 kHz) then was delivered to the tip electrode at 45 to 60 V when using a 7F/4-mm tip electrode (Cordis Webster) in 20 patients and 50 to 70 V when using an 8F/8-mm tip electrode (EP Technologies) in 10 patients (Table 3 \blacklozenge). Two adhesive electrosurgical dispersive pads (both positioned over the left posterior chest) were used for the return electrode. The ablation electrode was withdrawn toward the posteroapical margin of the coronary sinus ostium in 2- to 3-mm increments every 15 to 20 seconds while radiofrequency current was continuously applied (Fig 6A \blacklozenge and Fig 7A and 7B \blacklozenge). When the electrode entered the posteroapical edge of the coronary sinus ostium (Fig 7B \blacklozenge), the voltage was lowered to 45 to 50 V, and slight forward pressure (toward the tricuspid annulus) was applied to the catheter to enhance current delivery to the tissue between the coronary sinus ostium and the tricuspid annulus. When possible, radiofrequency current was delivered between the tricuspid annulus and the coronary sinus ostium as a single, continuous application. However, the application of radiofrequency current was terminated immediately in the event of an impedance rise ($\geq 10 \Omega$). In that event, two or more radiofrequency applications were required to produce the contiguous lesion. Voltage output was guided by impedance monitoring (avoiding more than 5- to 10- Ω decreases in impedance) to reduce the incidence of impedance rise.³⁵

Table 3. Ablation Results

View this table:
[In this window](#)
[In a new window](#)

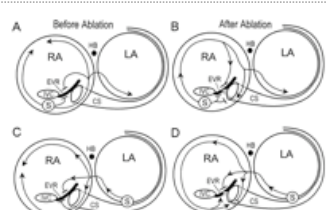
If atrial flutter persisted after one or more radiofrequency applications between the tricuspid annulus and the coronary sinus ostium, radiofrequency current was applied along the posterior margin of the coronary sinus ostium and between the posterior margin of the ostium and the eustachian ridge (Figs 6B and 7C \blacklozenge). If atrial flutter still persisted, radiofrequency current was applied along a line between the posterior or posterior paraseptal tricuspid annulus and the inferior vena cava or the eustachian ridge (Line PI in Fig 2C \blacklozenge and Fig 6C \blacklozenge).

This sequential approach, beginning with a lesion between the tricuspid annulus and the coronary sinus ostium, was used in 27 of the 30 patients. In the remaining 3 patients (Nos. 7, 19, and 24), radiofrequency current was only delivered between the posterior tricuspid annulus and the inferior vena cava or the eustachian valve/ridge (Fig 6C \blacklozenge). In 2 of these patients (Nos. 7 and 19) it was thought that elimination of the posterior input to the AV node (slow AV nodal pathway) by ablation of the septal isthmus might produce AV block. One of these patients (No. 7) had previously undergone an AV nodal modification procedure using the anterior approach, which might have eliminated the anterior inputs to the AV node (fast AV nodal pathway). The other patient (No. 19) had an A-H interval of 205 ms during sinus rhythm (and no retrograde AV nodal conduction) after a myomectomy for hypertrophic obstructive cardiomyopathy, which might have indicated the absence of conduction over the fast AV nodal pathway (anterior inputs to the AV node). The third patient (No. 24) had a persistent left superior vena cava inserting into the great cardiac vein. This was associated with a giant coronary sinus ostium that displaced the eustachian ridge to approximately 4 cm from the tricuspid annulus. In this patient, we believed that a continuous lesion could be created more reliably through the posterior isthmus than through the septal isthmus.

Criteria for Successful Ablation and Termination of the Ablation Procedure

In 12 patients, ablation success was defined by (1) the termination of atrial flutter during an application of radiofrequency current due to conduction block within the reentrant circuit at the ablation site and (2) the inability to reinduce atrial flutter for a period of at least 30 minutes by programmed stimulation of the right and left atria (from the posterior or posterolateral coronary sinus), including extensive burst pacing (noninduction criteria). Isoproterenol was used in the postablation testing in patients who required isoproterenol for induction of atrial flutter before ablation at a dose exceeding the preablation dose.

In 18 patients, ablation success was defined by (1) the noninduction criteria and (2) the demonstration of a line of bidirectional conduction block between the tricuspid annulus and the eustachian valve/ridge (line of block criteria). We verified complete conduction block between the tricuspid annulus and the eustachian ridge by pacing the right atrium adjacent to the posterior tricuspid annulus (posterior to the ablation line) and noting that atrial activation propagates around the tricuspid annulus in the clockwise direction (as viewed in the left anterior oblique projection), with late atrial activation at the right anterior septum (His bundle electrogram) and even later atrial activation in the proximal coronary sinus, even though the electrodes in the proximal coronary sinus are anatomically close to the pacing site (Fig 8A and 8B \blacklozenge), and by pacing the left atrium from the posterior coronary sinus and noting that atrial activation propagates around the tricuspid annulus in the counterclockwise direction as viewed in the left anterior oblique projection, with early atrial activation at the anterior septum (His bundle electrogram) and late atrial activation at the tricuspid annulus immediately posterior to the ablation line (Fig 8C and 8D \blacklozenge).



View larger version (37K):
[In this window](#)
[In a new window](#)

Figure 8. Schematics illustrate the pacing technique used to verify a complete arc of conduction block after ablation of the septal isthmus (gray lines in B and D). A, Right atrial pacing adjacent to the posterior tricuspid annulus before ablation results in atrial activation around the tricuspid annulus in both the clockwise and counterclockwise directions with relatively early atrial activation recorded in the His bundle and proximal coronary sinus electrograms. B, After ablation of the septal isthmus, producing a complete arc of conduction block from the tricuspid annulus to the CS ostium, eustachian ridge, and IVC. Right atrial pacing adjacent to the posterior tricuspid annulus results in atrial activation around the tricuspid annulus only in the clockwise direction with late atrial activation recorded in the HB electrogram and even later activation recorded from the proximal CS. C, Left atrial pacing from the proximal CS before ablation results in right atrial activation from the septum in both the clockwise and counterclockwise directions. D, After ablation, left atrial pacing from the proximal CS produces right atrial activation only in the counterclockwise direction with the latest atrial activation recorded immediately posterior to the ablation line. Abbreviations as in previous figures. S indicates atrial pacing site.

Postablation Management

Patients were electrocardiographically monitored until hospital discharge on the second day after ablation. A transesophageal echocardiogram was obtained on the day after ablation to exclude a thrombus at the ablation sites, pericardial effusion, and tricuspid valve injury. The patients received aspirin (325 mg daily) for 6 weeks. No patient received antiarrhythmic drug therapy after ablation until recurrence of atrial flutter or atrial fibrillation. Patients were followed by the investigators

or by the referring physician, and follow-up information was confirmed by telephone at the time of writing.

Statistical Analysis

Data are listed as mean±SD. The significance of the difference between the Δ return intervals at the various entrainment pacing sites was assessed by ANOVA, with Scheffe's method for pairwise comparisons. A χ^2 test was used to determine the significance of the difference in atrial flutter recurrence between the two criteria for successful ablation and the significance of the difference in the clinical occurrence of atrial fibrillation after ablation between the presence or absence of structural heart disease, atrial enlargement, and previously documented atrial fibrillation. The number of applications of radiofrequency current was compared between the patients with or without previous ablation failure and the presence or absence of an episode of atrial fibrillation after ablation using a two-tailed, unpaired *t* test. A value of $P < .05$ was considered statistically significant.

Results

Atrial flutter was present at the onset of the electrophysiological study in 11 of the 30 patients. The ECG exhibited the pattern of typical atrial flutter with a negative flutter wave in the inferior leads in 10 of these 11 patients. Reverse typical atrial flutter (defined later) with a positive flutter wave in the inferior leads was present in the remaining patient (No. 20), who had had clinical episodes of both typical and reverse typical flutter. In the other 19 patients, typical atrial flutter was induced by extrastimuli or burst atrial pacing from the right atrial appendage and/or the coronary sinus (Fig 9A➤). Isoproterenol (1 to 2 $\mu\text{g}/\text{min}$) was required for sustained atrial flutter in 6 patients (Table 2➤). In 4 patients (Nos. 22 and 25 through 27), sustained typical atrial flutter could not be maintained because of spontaneous termination or recurrent spontaneous degeneration to atrial fibrillation. Episodes of reverse typical atrial flutter also were induced in 7 patients before ablation. Episodes of reverse typical atrial flutter were induced in 3 additional patients after elimination of typical atrial flutter by ablation. Therefore, typical atrial flutter was studied in 29 patients and reverse typical atrial flutter in 10 patients. The atrial cycle length during typical atrial flutter was 242 ± 52 ms (Table 2➤). The atrial cycle length of reverse typical atrial flutter before ablation (7 patients) was 204 ± 23 ms. The atrial cycle length of reverse typical atrial flutter induced only after the elimination of typical atrial flutter by ablation (3 additional patients) was 235 ± 59 ms (Table 2➤). Sustained atrial fibrillation (≥ 60 seconds) was induced by programmed atrial stimulation in 10 patients before ablation and 2 patients after ablation of atrial flutter (Table 3➤).

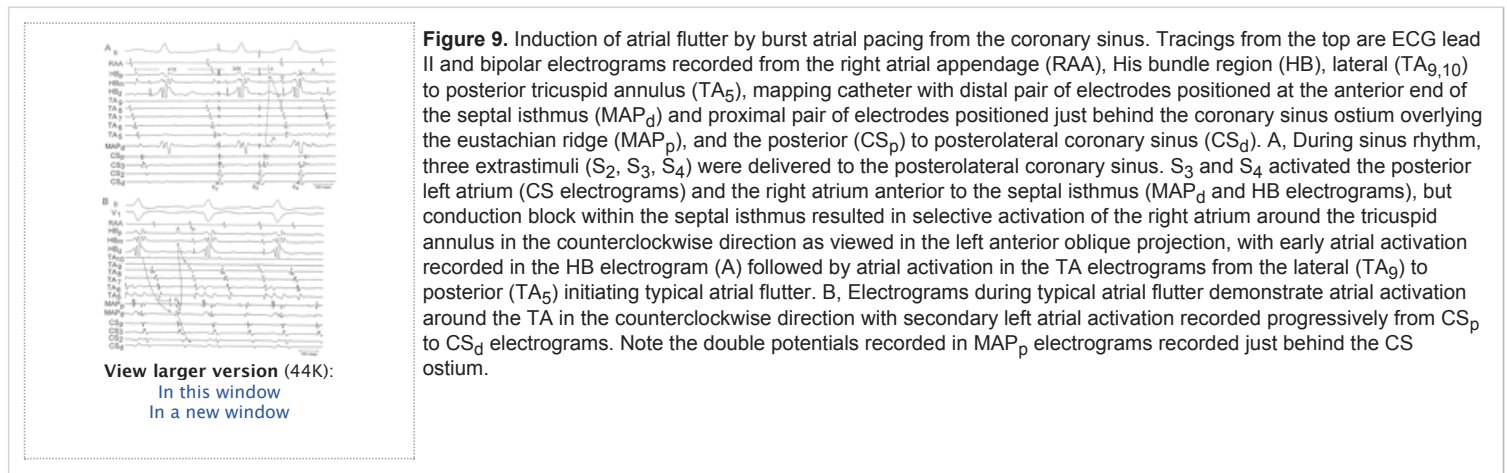
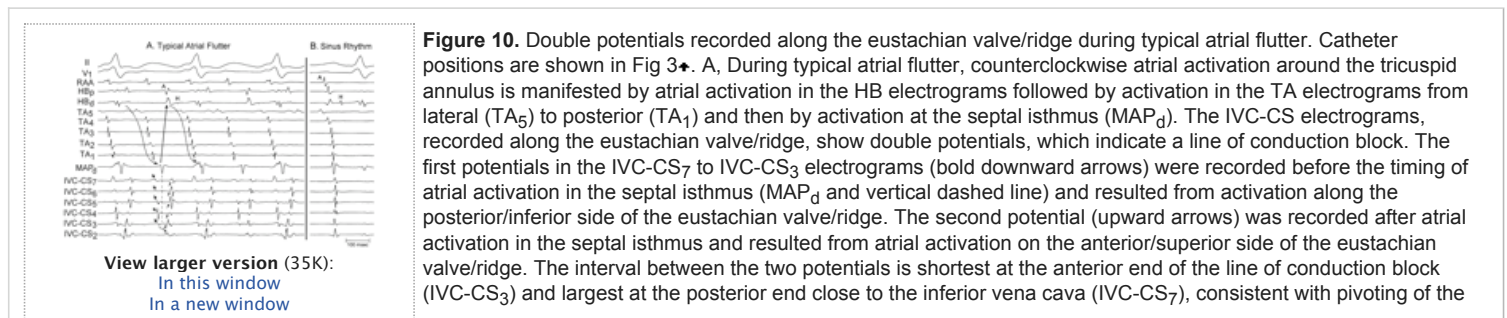


Table 2. Electrophysiological Characteristics of Atrial Flutter

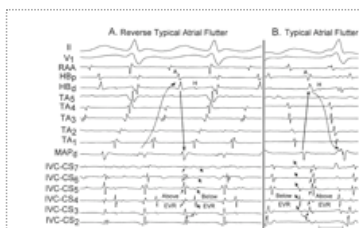
[View this table:](#)
[In this window](#)
[In a new window](#)

Endocardial Mapping

Recordings along the tricuspid annulus during typical atrial flutter showed atrial activation propagating around the tricuspid annulus in the counterclockwise direction as viewed in the left anterior oblique projection (anteriorly along the septum and posteriorly along the free wall) in all 29 patients (Figs 9 and 10A➤). Left atrial activation, recorded from the proximal coronary sinus, occurred soon after the timing of atrial activation in the septal isthmus (Fig 9B➤). Left atrial activation was recorded at progressively later times at more distal sites in the coronary sinus, consistent with activation of the left atrium in the counterclockwise direction as viewed in the left anterior oblique projection. During reverse typical atrial flutter, atrial activation propagated around the tricuspid annulus in the clockwise direction as viewed in the left anterior oblique projection (Fig 11➤).



wavefront around the anterior end of the eustachian ridge and the CS ostium. B, During sinus rhythm, electrograms along the eustachian valve/ridge (IVC-CS₇ to IVC-CS₃) did not exhibit distinct double potentials separated by an isoelectric interval. Abbreviations as in previous figures.



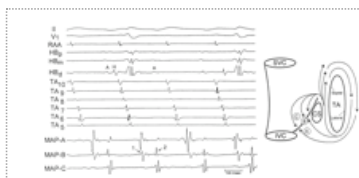
[View larger version \(39K\):](#)
[In this window](#)
[In a new window](#)

Figure 11. Relationship of double potentials between typical and reverse typical atrial flutter. Patient and catheter positions are the same as in Figs 3 and 10. A, During reverse typical atrial flutter, the atrial impulse propagated around the tricuspid annulus in the clockwise direction, reflected by atrial activation at the septal isthmus (MAP_d) followed by atrial activation at the posterior tricuspid annulus (TA₁) and lateral tricuspid annulus (TA₅), opposite to the pattern recorded during typical atrial flutter (B). Double potentials, separated by an isoelectric interval, were recorded along the eustachian valve/ridge (IVC-CS₃ to IVC-CS₇) during reverse typical atrial flutter. The first potential resulted from atrial activation anterior to the eustachian valve/ridge (Above EVR) and the second potential resulted from activation posterior to the eustachian valve/ridge (Below EVR). Note the order of the two potentials is opposite to the order in typical atrial flutter (B). Abbreviations as in previous figures.

Electrograms recorded from the septal isthmus, between the coronary sinus ostium and the tricuspid annulus, exhibited wide atrial potentials that often had multiple components but not discrete double potentials separated by isoelectrical interval (MAP_d electrogram in Fig 9B). Conduction block in the septal isthmus was responsible for the spontaneous termination of typical atrial flutter in 11 patients, which suggests that the septal isthmus may have a low safety factor for impulse propagation. Conduction block at this site in the anterior-to-posterior direction was responsible for the induction of typical atrial flutter by burst pacing from the coronary sinus in 6 patients (Fig 9A).

Double Potentials

Distinct double potentials separated by an isoelectrical interval (consistent with conduction block) were recorded along the eustachian valve/ridge from the anterior/superior margin of the coronary sinus ostium to the inferior vena cava in all 29 patients during typical atrial flutter (Figs 1, 3, and 10). The first of the two potentials was large and sharp and the second potential was small and rounded (distant) when the recording electrodes were positioned posterior/inferior to the line of equal amplitude double potentials, indicating a location proximal to (below) the line of block (MAP-A electrogram in Fig 12). The second of the two potentials was large and sharp and the first potential was small and distant when the recording catheter was positioned anterior/superior or distal to (above) the line of equal amplitude potentials (MAP-B electrogram in Fig 12), which suggests a location distal to (above) the line of block (MAP-C electrogram in Fig 12). Atrial activation in the septal isthmus between the tricuspid annulus and the coronary sinus ostium (site C in Fig 1) followed the timing of the first potential of the double potentials and preceded the second potential of the double potentials recorded along the eustachian valve/ridge (MAP electrogram in Fig 10). The timing of the second potential became progressively later from the coronary sinus end to the inferior vena cava end of the eustachian valve/ridge. The greatest interval between the two potentials (91±17 ms, Table 2) was consistently recorded near the inferior vena cava end of the eustachian valve/ridge. The second potential of the two potentials was usually recorded after atrial activation in the His bundle electrogram, which suggests that the second potential may represent activation outside of the reentrant circuit.

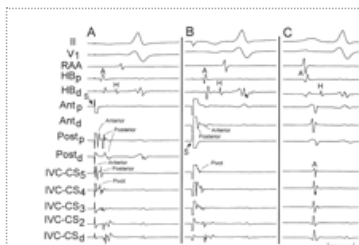


[View larger version \(24K\):](#)
[In this window](#)
[In a new window](#)

Figure 12. Characteristics of the double potentials recorded along the eustachian valve/ridge. The bottom three tracings are composed electrograms recorded at three sites shown schematically on the right (A, B, and C). MAP-B was recorded on the eustachian ridge. The two potentials of the double potential are approximately equal in amplitude. MAP-A was recorded on the posterior/inferior side of the eustachian ridge and exhibited a large, sharp first potential and a small, rounded second potential (representing far field activation on the anterior/superior side of the eustachian ridge). MAP-C was recorded anterior/superior to the eustachian ridge. The second potential is large and sharp, whereas the first potential is small and rounded (far field activation from the posterior/inferior side of the eustachian ridge). Abbreviations as in previous figures.

Double potentials also were recorded along the eustachian valve/ridge during reverse typical atrial flutter. The order of the two potentials was reversed (compared with typical flutter), with the first potential resulting from atrial activation anterior to (above) the eustachian valve/ridge and the second potential resulting from activation posterior to (below) the eustachian valve/ridge (Fig 11).

Double potentials were not recorded along the eustachian valve/ridge during sinus rhythm (Fig 10B). However, double potentials were consistently elicited by right atrial pacing at long cycle lengths just anterior or posterior to the eustachian valve/ridge, with activation occurring in the septal isthmus before activation of the opposite side of the eustachian valve/ridge (Figs 4 and 13).



[View larger version \(31K\):](#)
[In this window](#)

Figure 13. Evidence obtained by atrial pacing for fixed conduction block across the eustachian valve/ridge. Catheter positions are shown in Fig 4. The anterior (Ant) and posterior (Post) catheters are positioned just anterior and posterior to the eustachian valve/ridge, respectively. A, During atrial pacing from the distal pair of electrodes on the Ant catheter at a cycle length of 600 ms, the proximal pair of electrodes on the Post catheter (Post_p, located close to the eustachian valve/ridge) recorded two distinct potentials separated by an isoelectric interval. The first potential resulted from atrial activation anterior to the eustachian valve/ridge and the second (delayed) potential resulted from atrial activation posterior to the eustachian valve/ridge. The distal pair of electrodes on the Post catheter (Post_d) were located further from the eustachian valve/ridge and recorded only a single delayed potential. The IVC-CS₄ electrogram is recorded at the anterior margin of the coronary sinus ostium and shows atrial activation midway in timing between the anterior and posterior potentials recorded along the eustachian valve/ridge. B, During atrial pacing from the distal pair of electrodes on the Post catheter at a cycle length of 600 ms, the distal pair of electrodes

[In a new window](#)

on the Ant catheter (Ant_d, located close to the eustachian valve/ridge) recorded two atrial potentials separated by an isoelectric interval. The first potential resulted from atrial activation posterior to the eustachian valve/ridge, while the second (delayed) potential resulted from atrial activation anterior to the eustachian valve/ridge. During this recording, the IVC-CS₅ electrodes were located at the anterior margin of the coronary sinus ostium and recorded atrial activation midway in timing between posterior and anterior potentials recorded along the eustachian valve/ridge. The presence of double potentials along the eustachian valve/ridge during atrial pacing at a long cycle length provides strong evidence for fixed (not functional) conduction block. C, Distinct double potentials (separated by an isoelectric interval) were not recorded during sinus rhythm, indicating that atrial activation was occurring nearly simultaneously on both sides of the eustachian valve/ridge. Abbreviations as in previous figures.

Entrainment Pacing

Entrainment pacing (cycle length, 15 to 25 ms shorter than the flutter cycle length) at the septal isthmus, between the tricuspid annulus and the coronary sinus ostium, produced an atrial activation sequence that was identical to the flutter in all recorded electrograms (concealed entrainment) in each of the 15 patients tested. The Δ return interval (return interval minus flutter cycle length) at this pacing site was 0 to 15 ms (mean, 4.2 ± 4.3 ms) and ≤ 8 ms in 14 of the 15 patients (Fig 14A \blacklozenge and Table 2 \blacklozenge).



[View larger version \(43K\):](#)
[In this window](#)
[In a new window](#)

Figure 14. Entrainment pacing from the septal isthmus and anterior and posterior to the eustachian valve/ridge during typical atrial flutter. A, MAP electrograms were recorded from the septal isthmus between the tricuspid annulus and the coronary sinus ostium. The left tracing was recorded immediately before the onset of entrainment pacing. The tracing at the right shows the last 4 complexes of entrainment pacing at a cycle length of 215 ms from the distal pair of electrodes on the MAP catheter. The atrial activation sequence during entrainment pacing was identical to the atrial flutter. The return interval was 230 ms, equal to the atrial flutter cycle length (Δ return interval=0 ms). B, The MAP catheter was positioned just posterior to the eustachian valve/ridge, and the MAP_d electrogram during atrial flutter shows double potentials with a large, sharp first potential (left). Entrainment pacing at this site produced an atrial activation sequence around the tricuspid annulus that was identical to the atrial flutter activation sequence but was associated with a long return interval of 260 ms (Δ return interval=30 ms), which indicated that the pacing electrodes were located some distance from the reentrant circuit ("blind alley"). C, The MAP catheter was positioned anterior to the eustachian valve/ridge, and the MAP_d electrogram during atrial flutter shows double potentials, with a small (distant) first potential and a large second potential (left). Entrainment pacing at this site resulted in a longer return interval of 270 ms (Δ return interval=40 ms), indicating that the pacing site was located further from the reentrant circuit. Abbreviations as in previous figures.

Entrainment pacing just posterior to the eustachian valve/ridge, which corresponds to site B in Fig 1 \blacklozenge , produced an atrial activation sequence identical to the flutter but with a Δ return interval of 8 to 50 ms (mean, 30 ± 12 ms) and ≥ 15 ms in 14 of the 15 patients (Fig 14B \blacklozenge and Table 2 \blacklozenge). Entrainment pacing just anterior to the eustachian valve/ridge (site E in Fig 1 \blacklozenge) produced a Δ return interval of 15 to 60 ms (mean, 37 ± 13 ms) (Fig 14C \blacklozenge and Table 2 \blacklozenge).

Entrainment pacing from sites along the right atrial free wall adjacent to the tricuspid annulus produced some alternation of the atrial activation sequence close to the pacing site and alteration of the P wave. However, the Δ return interval was ≤ 8 ms in 14 of the 15 patients (Fig 15 \blacklozenge and Table 2 \blacklozenge). In the remaining patient (No. 23), the Δ return interval was 15 ms at all sites tested around the tricuspid annulus and at the septal isthmus.



[View larger version \(203K\):](#)
[In this window](#)
[In a new window](#)

Figure 15. Entrainment pacing at two sites along the free wall tricuspid annulus. Catheter positions are shown in C. A shows the last 4 complexes of entrainment pacing from the TA₈ bipolar electrode on the Halo catheter located at the anterolateral tricuspid annulus. Note that the return interval was 275 ms, identical to the atrial flutter cycle length (Δ return interval=0 ms). B shows the last 4 complexes of entrainment pacing from the TA₅ bipolar electrode on the Halo catheter located at the lateral tricuspid annulus. Entrainment pacing at this site also resulted in a return interval of 275 ms (Δ return interval=0 ms), indicating that these two sites around the tricuspid annulus were located within the reentrant circuit. Note that the A-A interval was 275 ms at all of the sites along the tricuspid annulus distal to the pacing site (TA₁ to TA₄ electrograms) and the A-A interval was equal to the pacing cycle length (260 ms) at sites along the tricuspid annulus proximal to the pacing site (HB, TA₈, and TA₇ electrograms). The IVC-CS₈ to IVC-CS₆ electrograms recorded atrial activation on the anterior side of the eustachian valve/ridge (second potential of the double potentials), while the IVC-CS₄ to IVC-CS₁ electrograms recorded atrial activation in the proximal coronary sinus. The MAP_d electrogram was recorded at the septal isthmus and exhibits a potential midway between the double potentials recorded on the IVC-CS₆ electrogram, while the MAP_p electrogram was recorded behind the coronary sinus ostium and exhibits a potential close in timing to the second potential of the double potentials in the IVC-CS₆ electrogram. C, Radiograph in the left anterior oblique projection showing the location of the catheter electrodes for A and B. Arrows indicate the location of 10 close bipolar electrodes on the Halo catheter positioned around the tricuspid annulus. Abbreviations as in previous figures.

Catheter Ablation

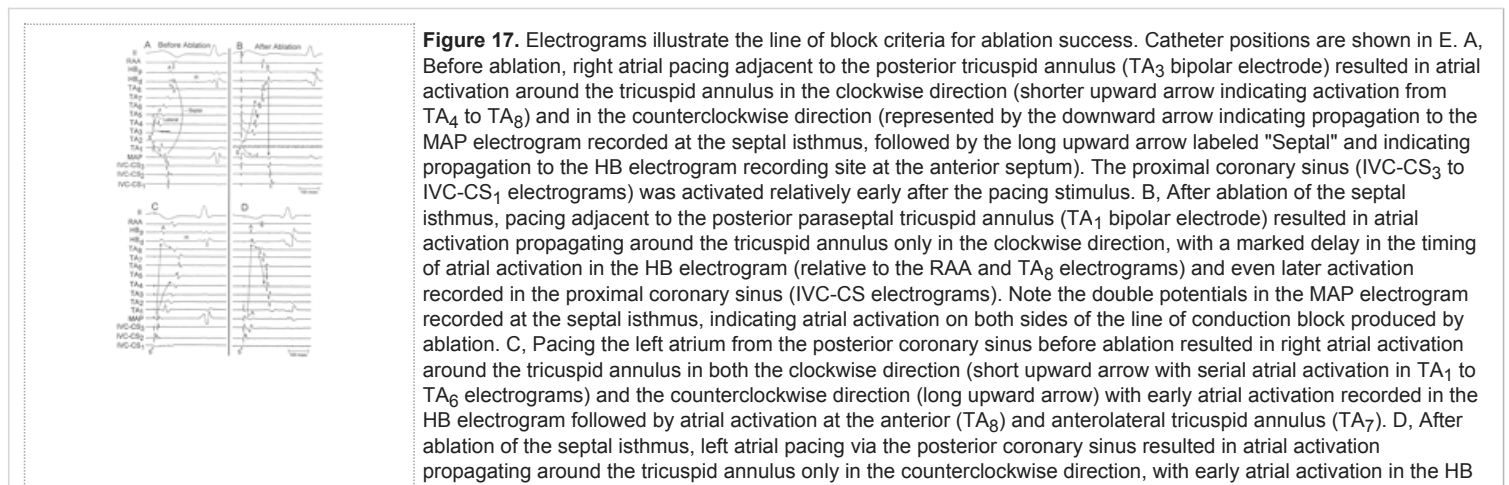
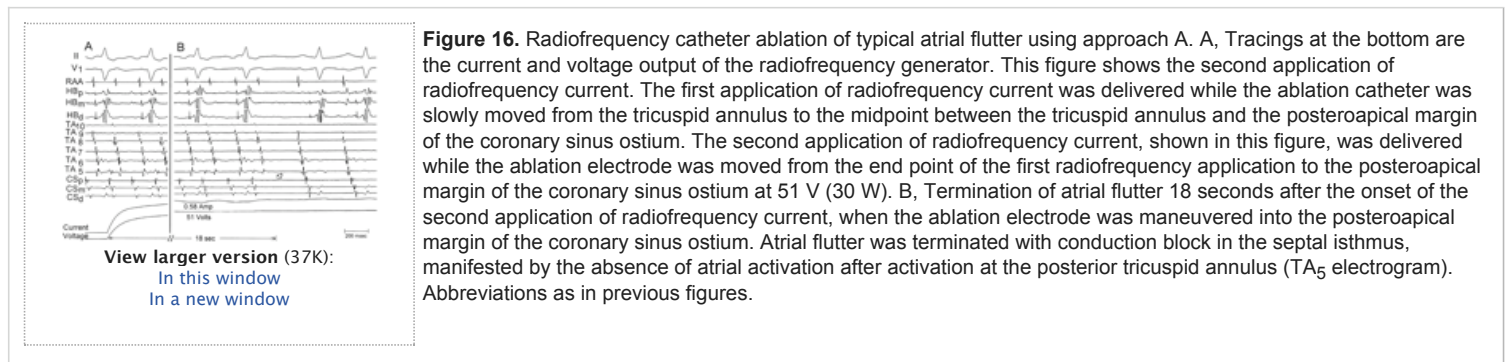
In 27 of the 30 patients, ablation was initiated with applications of radiofrequency current delivered along a line between the tricuspid annulus and the posteroapical margin of the coronary sinus ostium, as illustrated in Fig 6A♣ (approach A). Ablation only in this region eliminated atrial flutter in 14 of the 27 patients with 1 to 16 (median, 2) applications of radiofrequency current (column "A" in Table 3♣). Extending the ablation line to the eustachian ridge (including the posterior margin of the coronary sinus ostium), as illustrated in Fig 6B♣ (approach A and B), eliminated the atrial flutter in 12 additional patients (column "A and B" in Table 3♣). In 2 of these 12 patients (Nos. 9 and 10), typical atrial flutter was eliminated by ablation approach A, but reverse typical atrial flutter then was induced by programmed atrial stimulation. The reverse typical atrial flutter was eliminated by extending the ablation line to the eustachian ridge. Therefore, ablation using approach A or approach A and B eliminated typical and reverse typical atrial flutter in 26 of the 27 patients with 1 to 21 (median, 3; mean, 5.8 ± 5.5) applications of radiofrequency current. The one remaining patient (No. 16) required additional ablation between the tricuspid annulus and the inferior vena cava to eliminate atrial flutter (column "A, B, and C" in Table 3♣). This patient had a large coronary sinus ostium that was located more anteriorly than usual, and a His bundle potential was recorded at the anterior margin of the coronary sinus ostium. The unusual anatomy and our concern about the possibility of producing heart block significantly limited attempts to create a line of block between the tricuspid annulus and the coronary sinus ostium.

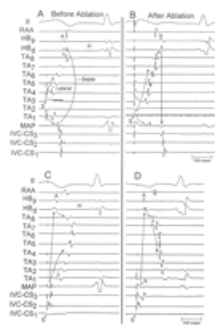
In 3 patients with either a high risk of AV block (patients 7 and 19) or a giant coronary sinus ostium caused by a persistent left superior vena cava inserting into the great cardiac vein (patient 24), ablation of atrial flutter was performed by delivery of radiofrequency current only between the posterior or posterior-paraseptal tricuspid annulus and the inferior vena cava or the eustachian ridge (Fig 6C♣ and column "C Only" in Table 3♣). Five to 12 applications of radiofrequency current were required to eliminate atrial flutter.

The number of applications of radiofrequency current required to eliminate atrial flutter was not significantly different for 7 patients with previous ablation failure (mean, 6.6 ± 5.9) compared with 23 patients without previous ablation procedures (mean, 6.7 ± 6.2 ; Tables 1 and 3♣).

Criteria for Ablation Success

In 12 patients, ablation was considered successful and the procedure was terminated when an application of radiofrequency current terminated the atrial flutter (Fig 16♣) and neither typical nor reverse typical atrial flutter was induced by programmed atrial stimulation (noninduction criteria, Table 3♣). In the remaining 18 patients, ablation was not considered successful until the noninduction criteria were met and a line of complete bidirectional conduction block was produced between the posteroseptal tricuspid annulus and the eustachian valve/ridge (line of block criteria, Table 3♣). The completion of the line of conduction block was verified by right atrial pacing adjacent to the posterior paraseptal tricuspid annulus (posterior to the ablation line) and by pacing the left atrium from the posterior coronary sinus (equivalent to a site anterior to the ablation line). During right atrial pacing adjacent to the posterior tricuspid annulus, a contiguous line of block eliminated early anterior and leftward propagation of the atrial impulse, manifested by propagation of the atrial impulse around the tricuspid annulus in the clockwise direction (as viewed in the left anterior oblique projection) with late activation at the anterior septum (His bundle electrogram) and even later activation of the posterior left atrium recorded from the proximal coronary sinus (Fig 8A and 8B♣♣ and Fig 17A, 17B, and 17E♣♣♣). A more striking shift in the pattern of atrial activation around the tricuspid annulus was observed during coronary sinus pacing. Before ablation, coronary sinus pacing resulted in activation of the right atrium in both the anterior and posterior directions, producing activation around the tricuspid annulus in both the counterclockwise and clockwise directions (Figs 8C and 17C♣♣). After completion of the line of conduction block, the right atrium was activated only in the anterior direction, which resulted in activation around the tricuspid annulus in only the counterclockwise direction (Figs 8D and 17D♣♣). The activation time at the posteroseptal right atrium (posterior to the ablation line) during coronary sinus pacing shifted from the earliest right atrial activation time before ablation to the latest time after ablation (Fig 17C and 17D♣♣).



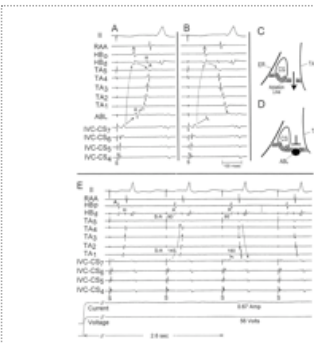


View larger version (184K):
[In this window](#)
[In a new window](#)

electrograms and later activation in the anterior (TA_8 electrogram), lateral (TA_5 electrogram), and posterior tricuspid annulus (TA_2 electrogram). Latest atrial activation was recorded at the posterior paraseptal tricuspid annulus (TA_1 electrogram) just posterior to the line of block across the septal isthmus. Note the two atrial potentials (double potentials) in the MAP electrogram. The findings in B and D confirm the presence of a complete arc of conduction block (extending from the tricuspid annulus to the coronary sinus ostium to the inferior vena cava), fulfilling the line of block criteria for ablation success. Abbreviations as in previous figures.

The presence of a complete line of conduction block was examined in 1 of the 3 patients in whom reverse typical atrial flutter was induced after elimination of typical atrial flutter by ablation (patient 9 in Table 3 \blacklozenge). Conduction across the ablation region was still present, manifested by early activation of the posterior right atrium adjacent to the tricuspid annulus during coronary sinus pacing. Extending the ablation line to the eustachian ridge was associated with the development of a complete line of conduction block and elimination of reverse typical atrial flutter.

In 15 of the 18 patients in whom line of block criteria were used to define ablation success, a line of conduction block was present as soon as the inducibility of typical and reverse typical atrial flutter was eliminated. In the remaining 3 patients (Nos. 28, 29, and 30), atrial flutter was terminated by the third to eighth application of radiofrequency current and neither forms of atrial flutter could be induced, but some degree of conduction across the ablation region was still present during pacing from the posterior right atrium (adjacent to the tricuspid annulus) or coronary sinus. In these 3 patients, the defect in the line of conduction block was found by pacing from the coronary sinus and mapping just posterior to the ablation line to locate an early atrial potential (Fig 18A and 18C \blacklozenge). Ablation at that site was followed by a shift in the atrial activation sequence along the posterior tricuspid annulus from the clockwise direction to the counterclockwise direction as viewed in the left anterior oblique projection (Fig 18B, 18D, and 18E \blacklozenge). Importantly, neither typical nor reverse typical atrial flutter was induced after the completion of the line of conduction block in any of the 18 patients.



View larger version (41K):
[In this window](#)
[In a new window](#)

Figure 18. Use of mapping to identify the defect in an incomplete ablation line across the septal isthmus. A, After 14 applications of radiofrequency current across the septal isthmus, the posterior margin of the coronary sinus ostium, and between the coronary sinus ostium and the eustachian ridge (ER), left atrial pacing from the posterior coronary sinus showed delayed (but not blocked) conduction to the posterior tricuspid annulus (TA_1 electrogram). Mapping posterior to the ablation line with the ablation catheter (ABL electrogram) identified an early atrial potential (A) posterior to the septal isthmus, indicating the site of the defect in the ablation line, as shown schematically by the arrow in C. E, Ablation at this site resulted in an abrupt shift in the atrial activation sequence around the tricuspid annulus, with an increase in the stimulus-atrial (S-A) interval at the posterior tricuspid annulus (TA_1 electrogram) from 145 to 180 ms, indicating the development of complete block between the tricuspid annulus and the eustachian ridge. B, After ablation, pacing from the posterior coronary sinus results in atrial activation around the tricuspid annulus only in the counterclockwise direction with early atrial activation recorded in the HB electrograms and later activation at the posterior tricuspid annulus (TA_1 electrogram). Atrial activation was recorded latest in the ABL electrogram (small downward arrow), indicating completion of the line of conduction block as illustrated schematically in D. Abbreviations as in previous figures.

In 1 of the 12 patients (No. 7) in whom the noninduction criteria were used to define ablation success, conduction across the ablation line was still present after the fifth application of radiofrequency current despite noninducibility of atrial flutter. No further applications of radiofrequency current were delivered.

In 4 patients, ablation could not be performed during atrial flutter because of either frequent spontaneous termination of atrial flutter (patients 25 and 27) or frequent spontaneous conversion of atrial flutter to atrial fibrillation (patients 22 and 26). Ablation was performed during left atrial pacing from the posterior coronary sinus until a line of conduction block was evident by the abrupt delay in the timing of atrial activation at the posteroseptal tricuspid annulus (posterior to the eustachian valve/ridge) with a shift in the atrial activation sequence along the lateral and posterior tricuspid annulus from the clockwise direction to the counterclockwise direction as viewed in the left anterior oblique projection (Fig 18E \blacklozenge). Complete bidirectional block between the tricuspid annulus and the eustachian valve/ridge was confirmed by pacing the right atrium adjacent to the posterior tricuspid annulus (posterior to the ablation site) and noting a marked delay in the timing of atrial activation at the anteroseptal tricuspid annulus (His bundle region) and posteroseptal left atrium recorded from the coronary sinus (Fig 17B \blacklozenge).

Follow-up

The 30 patients have been followed for 3 to 60 months (mean, 19.7 ± 16.7 months). Atrial flutter recurred at 1 and 5 months in 2 (17%) of the 12 patients (Nos. 6 and 7) in whom the noninduction criteria were used to define ablation success (mean follow-up of 33.9 ± 16.3 months, Table 3 \blacklozenge). This includes the patient (No. 7) in whom complete conduction block was shown to be absent at the end of the procedure despite noninducibility of atrial flutter. The presence or absence of a line of conduction block was not determined in the other patient (No. 6) who had a recurrence of atrial flutter. In contrast, atrial flutter has not recurred in any of the 18 patients ($P < .1$) in whom ablation was continued until the line of block criteria were fulfilled (mean follow-up of 10.3 ± 8.3 months, Table 3 \blacklozenge).

At least one episode of atrial fibrillation occurred 2 days to 2 months after ablation in 8 (27%) of the 30 patients (Table 3 \blacklozenge). Compared with the 22 patients without atrial fibrillation after ablation, these 8 patients had a significantly greater incidence of structural heart disease (8 of 8 versus 14 of 22, $P < .05$), left or right atrial

enlargement (8 of 8 versus 7 of 22, $P < .01$), and a documented episode of atrial fibrillation before ablation (6 of 8 versus 6 of 22, $P < .05$; Tables 1 and 3 \blacklozenge). Atrial fibrillation occurred after ablation in 6 of the 8 patients who had the combination of atrial enlargement (left or right) and a previously documented episode of atrial fibrillation compared with only 2 of the 22 patients without both of these risk factors ($P < .01$). Patients who had an episode of atrial fibrillation after ablation required a significantly larger number of applications of radiofrequency current (7 to 21; median, 11; mean, 12.1 ± 4.9 applications versus 1 to 22; median, 3; mean, 5.8 ± 5.8 applications; $P < .05$).

Complications

There were no acute or late complications of the ablation procedure. Transesophageal echocardiography performed after ablation in all 30 patients showed no intracardiac thrombus, pericardial effusion, or injury to the tricuspid valve.

Discussion

This study examined the hypothesis that the eustachian valve/ridge forms a line of conduction block in typical atrial flutter between the inferior vena cava and the coronary sinus ostium that forces the reentrant impulse emerging from the posterior isthmus (between the tricuspid annulus and the inferior vena cava²¹) to propagate through the septal isthmus, between the tricuspid annulus and the coronary sinus ostium. The results of this study strongly support this hypothesis, including the recording of double potentials along the eustachian valve/ridge during typical and reverse typical atrial flutter, the response to pacing on either side of the eustachian valve/ridge, and the creation of an arc of conduction block extending from the tricuspid annulus to the coronary sinus ostium and the inferior vena cava by catheter ablation of the septal isthmus, eliminating atrial flutter.

Conduction Block Along the Eustachian Valve/Ridge

Waldo and other investigators^{19 20 24 25 26 27 28 29} have shown that a line of conduction block in the atrium is manifested by double potentials separated by an isoelectric interval. The first potential results from the arrival of the atrial impulse on one side of the line of block, whereas the second potential results from the later atrial activation on the other side of the line of block. In this study, double potentials were recorded during typical and reverse typical atrial flutter along a line extending from the region behind (and superior to) the coronary sinus ostium to the inferior vena cava in all 30 patients (Figs 9 through 12 \blacklozenge). Using intracardiac echocardiography, Olgin et al³⁶ recently showed that the line of double potentials corresponded to the anatomic location of the eustachian valve/ridge (Fig 2 \blacklozenge). The first potential of the double potentials during typical atrial flutter was large and sharp in electrograms recorded immediately posterior and inferior to the eustachian valve/ridge and was small and rounded (distant appearing) in recordings anterior and superior to the eustachian valve/ridge, whereas the second potential was large and sharp in recordings immediately anterior and superior to the eustachian valve and was small and rounded in recordings posterior and inferior to the eustachian valve/ridge (Fig 12 \blacklozenge). The interval between the double potentials was bridged uninterruptedly by recordings along the septal isthmus (from posterior to anterior) and then around the anterior margin of the coronary sinus ostium (in the counterclockwise direction as viewed in the right anterior oblique projection; Fig 10 \blacklozenge). This is consistent with arrival of the reentrant wavefront at the posterior/inferior side of the line of conduction block along the eustachian valve/ridge (first potential) followed by pivoting of the wavefront around the anterior margin of the coronary sinus ostium to activate the atrium on the anterior/superior side of the eustachian valve/ridge (second potential), as illustrated schematically in Fig 1 \blacklozenge . The observation that the interval between the two potentials of the double potentials is greatest in recordings close to the inferior vena cava (posterior end of the eustachian valve/ridge) supports the concept that the impulse propagates around the anterior end of the eustachian valve/ridge. Importantly, recordings from the septal isthmus (between the tricuspid annulus and the coronary sinus ostium) did not exhibit distinct double potentials (MAP_d electrogram in Fig 9 \blacklozenge and MAP electrogram in Fig 10 \blacklozenge) because the line of conduction block extends behind (superior to) the coronary sinus ostium, which is relatively far from the recording electrodes (Fig 1 \blacklozenge).

The line of conduction block along the eustachian valve/ridge also was present before induction of atrial flutter. During atrial pacing at rates just slightly faster than the sinus rate on either side of the eustachian valve/ridge, double potentials were recorded along the eustachian valve/ridge with late atrial activation on the opposite side (Figs 4, 5, and 13 \blacklozenge), indicating the presence of fixed anatomic block as opposed to functional block during atrial flutter. The finding of fixed block might be expected because the eustachian ridge contains primarily connective tissue, including the tendon of Todaro, with variable components of muscle. A line of fixed anatomic block also might be expected in patients without atrial flutter, but this remains to be examined.

Distinct double potentials were not recorded during sinus rhythm (Figs 10B and 13C \blacklozenge). The absence of double potentials indicates that the right atrium on both sides of the eustachian valve/ridge is activated nearly simultaneously during sinus rhythm. This may result from activation by a single wavefront propagating relatively parallel to the eustachian valve/ridge²⁷ but could result also from the simultaneous arrival of multiple wavefronts.

The response to ablation of the septal isthmus provides additional evidence of preexisting, fixed anatomic conduction block along the eustachian valve/ridge. After completion of the ablation line between the tricuspid annulus and the coronary sinus ostium or the eustachian ridge, pacing the right atrium posterior to the ablation line failed to activate the atrium on the other side of the ablation line and the posteroseptal left atrium until after the paced atrial impulse propagated around the tricuspid annulus in the clockwise direction as viewed in the left anterior oblique projection (Fig 8A and 8B \blacklozenge). Similarly, pacing the posterior left atrium from the coronary sinus resulted in early activation of the right atrium anterior to the ablation line and anterior/superior to the eustachian valve/ridge, but conduction block along the eustachian valve/ridge prevented activation of the right atrium immediately posterior to the ablation line until the atrial impulse propagated completely around the tricuspid annulus in the counterclockwise direction (Fig 8C and 8D \blacklozenge). Therefore, the ablation line between the tricuspid annulus and the eustachian valve/ridge, combined with preexisting conduction block along the eustachian valve/ridge, form a complete arc of conduction block extending from the tricuspid annulus to the coronary sinus ostium and to the inferior vena cava.

The preexisting line of conduction block along the eustachian valve/ridge appeared to extend to the coronary sinus ostium in 8 of the 16 patients in whom the line of block criteria were used, since ablation just along the septal isthmus (approach A) produced the complete arc of conduction block in these patients (Table 3 \blacklozenge). Conduction between the eustachian ridge and the coronary sinus ostium may have been present in the remaining half of the 16 patients (dashed arrow in Fig 6B \blacklozenge), since extension of the ablation line to the eustachian ridge was required to complete the arc of conduction block. The presence or absence of conduction block between the eustachian ridge and the coronary sinus ostium may be a reflection of the variability in the anatomic relationship between the connective tissue of the eustachian ridge and the thebesian valve of the coronary sinus ostium, as illustrated in Fig 2 \blacklozenge .

Reentrant Circuit in Atrial Flutter

Entrainment pacing is a powerful tool to determine whether a region of myocardium is located within the reentrant circuit of a tachycardia.^{30 31 32 33 34} Entrainment pacing within the septal isthmus produced an atrial activation sequence identical to the atrial flutter (concealed entrainment) and had a Δ return interval that was only 0 to 8 ms in 14 of the 15 patients tested. The combination of concealed entrainment and minimal Δ return interval provides strong evidence that the septal isthmus is located in the reentrant circuit of the typical atrial flutter. In the one remaining patient (No. 23), the Δ return interval was slightly longer at 15 ms. However, the Δ return interval also was 15 ms at 5 other sites around the tricuspid annulus, which suggests that the longer Δ return interval resulted from a conduction delay within the reentrant circuit produced by the faster pacing rate rather than that the septal isthmus is located outside of the reentrant circuit in this patient.

Entrainment pacing at sites immediately posterior/inferior to the eustachian valve/ridge also produced an atrial activation sequence identical to the atrial flutter with the exception of the region close to the pacing site, but the Δ return interval was longer at 8 to 50 ms (mean of 30 ± 12 ms) and ≥ 15 ms in 14 of the 15 patients tested (Fig 14B \blacklozenge and Table 2 \blacklozenge). The presence of concealed entrainment with prolonged Δ return interval suggests that this atrial myocardium is a "blind alley" connected to the reentrant circuit. However, in patients in whom atrial flutter continues after ablation of the septal isthmus (approach A), which is presumably caused by persistence of conduction between the eustachian ridge and coronary sinus ostium, this site may become part of the reentrant circuit (dashed arrow in Fig 6B \blacklozenge). This might be verified in future studies by entrainment pacing at sites below the eustachian valve/ridge after failure to eliminate atrial flutter by ablation of the septal isthmus. The single patient (No. 29) with a short Δ return interval of 8 ms did require ablation between the coronary sinus ostium and the eustachian ridge, which suggests that a shorter Δ return interval could identify patients with conduction between the coronary sinus ostium and the eustachian ridge during atrial flutter. However, several other patients who required ablation between the coronary sinus ostium and the eustachian ridge to complete the arc of conduction block had a relatively long Δ return interval (26 to 50 ms) following pacing at sites posterior/inferior to the eustachian valve/ridge (Table 2 \blacklozenge). Factors that might lead to a longer Δ return interval despite conduction between the coronary sinus ostium and the eustachian ridge include the distance between the eustachian valve/ridge and the tricuspid annulus and the size of the coronary sinus ostium (Fig 2 \blacklozenge). The atrial myocardium immediately anterior/superior to the eustachian valve/ridge does not appear to be part of the atrial flutter reentrant circuit because entrainment pacing in this region is associated with a long Δ return interval (mean, 37 ± 13 ms). The response to entrainment pacing and the ablation confirm the hypothesis of this study that the eustachian valve/ridge and the tricuspid annulus form the boundaries of a protected channel in the reentrant circuit of atrial flutter. The entrance to the channel is formed by the posterior isthmus (between the tricuspid annulus and the inferior vena cava) and its exit from the channel is formed by the narrower septal isthmus (between the tricuspid annulus and the coronary sinus ostium). Counter to the original hypothesis is that the reentrant impulse also may be able to exit between the coronary sinus ostium and the eustachian ridge in approximately half of the patients.

The remainder of the reentrant circuit is less clearly defined. Entrainment pacing at free wall sites around the tricuspid annulus was associated with a Δ return interval of 0 to 15 ms and no more than 6 ms longer than the Δ return interval at the septal isthmus in any of the 15 patients tested (Table 2 \blacklozenge). This suggests that the reentrant impulse in typical atrial flutter continues around the tricuspid annulus in the counterclockwise direction as viewed in the left anterior oblique projection. Previous studies have shown another line of conduction block (double potentials) in the region of the venae cavae.^{19 20} Using intracardiac echocardiography to identify the anatomic location of the recording catheter electrodes, Olgin et al³⁶ found that this line of conduction block was located along the crista terminalis. It is possible that reentry occurs simultaneously around the tricuspid annulus and the anterior margin of the crista terminalis in figure of 8, with the channel formed between the eustachian valve/ridge and the tricuspid annulus being common to both loops.³⁷

Implication for Catheter Ablation

The observation that the channel between the eustachian valve/ridge and the tricuspid annulus forms a protected component of the reentrant circuit suggests that typical and reverse typical atrial flutter can be eliminated by creation of a perpendicular line of ablation at any site along the channel from the posterior isthmus to the septal isthmus (Fig 6 \blacklozenge). The potential advantages of ablation at the septal isthmus as opposed to the posterior isthmus include the shortest distance across the funnel-shaped channel and the smooth surface compared with the irregular surface of the pectinate muscle in the posterior isthmus (Fig 2C \blacklozenge). This study showed that typical flutter and reverse typical atrial flutter were eliminated in 26 of the 27 patients by ablation of the septal isthmus with 1 to 21 (median, 3) applications of radiofrequency current. This required ablation only between the tricuspid annulus and the coronary sinus ostium (approach A) in 14 of the 26 patients and required extension of the ablation line to the eustachian ridge in the remaining 12 patients (approach A and B). In a single patient (No. 16), more posterior ablation in the channel was required to eliminate atrial flutter that was due to an unusually anterior location of the coronary sinus ostium and its proximity to the His bundle (and therefore the AV node). These results compare favorably, in terms of overall success rate and number of applications of radiofrequency current, with previous studies that target the posterior isthmus for ablation.^{21 22 23} Importantly, both approaches are effective and safe, and one or the other may be preferable in individual patients. In this study, ablation at the posterior isthmus was performed for 3 patients who were considered to be at risk of AV nodal block associated with ablation of the posterior input to the AV node (slow AV nodal pathway) or who had a giant coronary sinus ostium associated with a persistent left superior vena cava.

Criteria for Ablation Success

An important finding in this study is that one or more applications of radiofrequency current may terminate atrial flutter and prevent its reinduction by extensive programmed right and left atrial stimulation without completing a line of conduction block between the tricuspid annulus and the eustachian valve/ridge. This was observed in 3 of the 14 (21%) patients in whom ablation was performed during atrial flutter and the line of block criteria were used for ablation success. This is approximately the same incidence of recurrence of atrial flutter (15% to 20%) after elimination of the inducibility of atrial flutter as in previous reports.^{18 21 22 23} In the present study, atrial flutter recurred in 2 of 12 (17%) patients in whom only the noninduction criteria were required for ablation success (Table 3 \blacklozenge). In the 2 patients who had recurrence of atrial flutter after seemingly successful ablation by the noninduction criteria, the line of block criteria were not fulfilled (ie, conduction was present across the ablation line) in one patient and not examined in the other. These observations strongly suggest that the line of block criteria are superior to the noninduction criteria to predict long-term ablation success of atrial flutter. The completion of the ablation-induced line of conduction block between the tricuspid annulus and the eustachian valve/ridge is quickly and easily identified by pacing the posterior or posterior paraseptal right atrium adjacent to the tricuspid annulus just posterior to the ablation line and by pacing the posterior left atrium from the coronary sinus. This technique also can be used with ablation of the posterior isthmus by placing the catheter electrodes posterior or lateral to the ablation line (Table 3 \blacklozenge). Identification of the line of block by coronary sinus pacing has been described recently in an animal model of atrial flutter and in a preliminary clinical report.^{38 39}

An important advantage of the line of block criteria is the ability to perform ablation without requiring atrial flutter during the application of radiofrequency current. In 4 of the 30 (13%) patients, atrial flutter could not be maintained for ablation because of either frequent spontaneous termination of atrial flutter (2 patients) or frequent spontaneous conversion from atrial flutter to atrial fibrillation (2 patients). We performed ablation during left atrial pacing from the proximal coronary sinus in these 4

patients using the shift in atrial activation along the posterior tricuspid annulus from the clockwise direction to the counterclockwise direction to identify ablation success. Ablation during coronary sinus pacing also was used to complete the line of conduction block in the 3 patients with persistence of conduction across the ablation line after elimination of the inducibility of atrial flutter (patients 28 to 30, Table 3 \blacklozenge). Mapping immediately posterior to the ablation line during coronary sinus pacing was used to identify the residual area of conduction through the ablation line (Fig 18 \blacklozenge). The ability to recognize ablation success without requiring the induction of atrial flutter either before or after ablation may significantly shorten total procedure time and fluoroscopy time as well as increase the long-term ablation success rate for typical and reverse typical atrial flutter.

Occurrence of Atrial Fibrillation After Ablation of Atrial Flutter

Previous studies of catheter ablation of atrial flutter have shown a high occurrence of atrial fibrillation after ablation.^{21 22 23 40} In this study, at least one episode of atrial fibrillation occurred during follow-up in 8 of the 30 (27%) patients (Table 3 \blacklozenge). Compared with the 22 patients without subsequent atrial fibrillation, these 8 patients had a higher incidence of major structural heart disease, right or left atrial enlargement, and previously documented episodes of atrial fibrillation. They also received a greater number of applications of radiofrequency current. The combination of right or left atrial enlargement and a history of atrial fibrillation was a strong predictor of subsequent occurrence of atrial fibrillation (6 of the 8 patients with this combination compared with 2 of the 22 patients without these two risk factors, $P < .01$). Ablation of atrial flutter still may be helpful in this group of patients since atrial fibrillation and/or the ventricular response rate may be tolerated better by the patient or better controlled pharmacologically. It is unclear whether the larger number of applications of radiofrequency current in the patients with subsequent atrial fibrillation (median, 11 versus 3) is causally related to the atrial fibrillation or simply a reflection of the increased difficulty in performing ablation in this group of patients with greater structural heart disease and dilated atria.

Conclusions

The eustachian valve/ridge forms a line of conduction block extending from the inferior vena cava to the coronary sinus ostium, which, combined with the tricuspid annulus, forms a protected channel within the reentrant circuit of typical and reverse typical atrial flutter. The posterior end of this channel forms the posterior isthmus (between the inferior vena cava and the tricuspid annulus) and its anterior end forms the septal isthmus (between the coronary sinus ostium and the tricuspid annulus). Ablation of the septal isthmus was found to be highly successful in eliminating typical and reverse typical atrial flutter, although extension of the ablation line to the eustachian ridge was required in half of the patients. This study describes a new technique for defining ablation success by confirming that the ablation line has produced a complete arc of conduction block extending from the tricuspid annulus to the coronary sinus ostium and the inferior vena cava. This new criteria for ablation success may reduce the recurrence of atrial flutter after seemingly successful ablation and also allow successful ablation without requiring the presence of atrial flutter at the time of ablation.

Acknowledgments

This study was supported by a grant from the National Institutes of Health (R01-HL-39670) and a grant from the Oklahoma Center for the Advancement of Science and Technology (HRC-RRP-A-028).

Footnotes

Presented in part at the 14th Annual Scientific Sessions of the North American Society of Pacing and Electrophysiology, May 1993, San Diego, Calif.

Received September 5, 1995; revision received December 18, 1995; accepted December 19, 1995.

References

1. Jolly WA, Ritchie. Auricular flutter and fibrillation. *Heart*. 1911;2:177-221.
2. Lewis T, Feil HS, Stroud WD. Observations upon flutter and fibrillation, II: the nature of auricular flutter. *Heart*. 1920;7:191-245.
3. Rosenblueth A, Garcia-Ramos J. Studies on flutter and fibrillation, II: the influence of artificial obstacles on experimental auricular flutter. *Am Heart J*. 1947;33:677-684.[[Medline](#)] [[Order article via Infotrieve](#)]
4. Puech P, Latour H, Grolleau R. Le flutter et ses limites. *Arch Mal Coeur*. 1970;61:116-144.
5. Waldo AL, McLean WAH, Karp RB, Kouchoukos NT. Entrainment and interruption of atrial flutter with atrial pacing: studies in man following open heart surgery. *Circulation*. 1977;56:737-745.[[Abstract/Free Full Text](#)]
6. Wells JL, McLean WAH, James TN, Waldo AL. Characterization of atrial flutter: studies in man after open heart surgery using fixed atrial electrodes. *Circulation*. 1979;60:665-673.[[Free Full Text](#)]
7. Boineau JP, Schuessler RB, Mooney CR, Miller CB, Wild AC, Hudson RD, Borremano JM, Brockno CW. Natural and evoked atrial flutter due to circus movement in dogs. *Am J Cardiol*. 1980;45:1167-1181.[[Medline](#)] [[Order article via Infotrieve](#)]
8. Inoue H, Matsuo H, Takayanagi K, Murao S. Clinical and experimental studies of the effects of atrial extrastimulation and rapid pacing on atrial flutter cycle: evidence of macro-reentry with an excitable gap. *Am J Cardiol*. 1981;48:623-631.[[Medline](#)] [[Order article via Infotrieve](#)]
9. Disertori M, Inama G, Vergara G, Guarnerio M, Del Favero A, Furlanello F. Evidence of a reentry circuit in the common type of atrial flutter in man. *Circulation*. 1983;67:434-440.[[Abstract/Free Full Text](#)]
10. Frame LH, Page RL, Hoffman BF. Atrial reentry around an anatomic barrier with a partially refractory excitable gap: a canine model of atrial flutter. *Circ Res*. 1986;58:495-511.[[Abstract/Free Full Text](#)]

11. Klein GJ, Guiraudon GM, Sharma AD, Milstein S. Demonstration of macroreentry and feasibility of operative therapy in the common type of atrial flutter. *Am J Cardiol.* 1986;57:587-591.[\[Medline\]](#) [\[Order article via Infotrieve\]](#)
12. Beckman K, Ta-Lin H, Krafchek J, Wyndham CRC. Classic and concealed entrainment of typical and atypical atrial flutter. *PACE.* 1986;9:826-835.
13. Frame LH, Page RL, Boyden PA, Fenoglio JJ, Hoffman BF. Circus movement in the canine atrium around the tricuspid ring during experimental atrial flutter and during reentry in vitro. *Circulation.* 1987;76:1155-1175.[\[Abstract/Free Full Text\]](#)
14. Boyden PA. Activation sequence during atrial flutter in dogs with surgically induced right atrial enlargement, I: observations during sustained rhythm. *Circ Res.* 1988;62:596-608.[\[Abstract/Free Full Text\]](#)
15. Fujimoto T, Inoue T, Fukuzaki H. Characterization of slow conduction in the common type of atrial flutter: using transient entrainment. *Jpn Circ J.* 1989;54:237-244.
16. Saoudi N, Atallah G, Kirkorian G, Touboul P. Catheter ablation of the atrial myocardium in human type I atrial flutter. *Circulation.* 1990;81:762-771.[\[Abstract/Free Full Text\]](#)
17. Cox JL, Schuessler RB, Boineau JP. The surgical treatment of atrial fibrillation, I: summary of the current concepts of the mechanisms of atrial flutter and atrial fibrillation. *J Thorac Cardiovasc Surg.* 1991;101:402-405.[\[Abstract\]](#)
18. Feld GK, Fleck RP, Chen P-S, Boyce K, Bahnson TD, Stein JB, Calisi CM, Ibarra M. Radiofrequency catheter ablation for the treatment of human type 1 atrial flutter: identification of a critical zone in the reentrant circuit by endocardial mapping techniques. *Circulation.* 1992;86:1233-1240.[\[Abstract/Free Full Text\]](#)
19. Cosio FG, Arribas F, Barbero JM, Kallmeyer CK, Goicolea A. Validation of double-spike electrograms as markers of conduction delay or block in atrial flutter. *Am J Cardiol.* 1988;61:775-780.[\[Medline\]](#) [\[Order article via Infotrieve\]](#)
20. Olshansky B, Okumura K, Henthorn RW, Waldo AL. Characterization of double potentials in human atrial flutter: studies during transient entrainment. *J Am Coll Cardiol.* 1990;15:833-841.[\[Abstract\]](#)
21. Cosio FG, Lopez-Gil M, Goicolea A, Arribas F, Barroso JL. Radiofrequency ablation of the inferior vena cava-tricuspid valve isthmus in common atrial flutter. *Am J Cardiol.* 1993;71:705-709.[\[Medline\]](#) [\[Order article via Infotrieve\]](#)
22. Lesh MD, Van Hare GF, Epstein LM, Fitzpatrick AP, Scheinman MM, Lee RJ, Kwasman MA, Grogan HR, Griffin JC. Radiofrequency catheter ablation of atrial arrhythmias: results and mechanisms. *Circulation.* 1994;89:1074-1089.[\[Abstract/Free Full Text\]](#)
23. Kirkorian G, Moncada E, Chevalier P, Canu G, Claudel JP, Bellon C, Lyon L, Touboul P. Radiofrequency ablation of atrial flutter: efficacy of an anatomically guided approach. *Circulation.* 1994;90:2804-2814.[\[Abstract/Free Full Text\]](#)
24. Nakagawa H, Wang X, McClelland J, Beckman K, Lazzara R, Hazlitt A, Arruda M, Santoro I, Abdalla I, Singh A, Sweidan R, Gossinger H, Hirao K, Widman L, Jackman W. Line of conduction block extends from inferior vena cava to coronary sinus ostium in common atrial flutter. *PACE.* 1993;16:881. Abstract.
25. Nakagawa H, McClelland J, Beckman K, Wang X, Lazzara R, Hazlitt A, Santoro I, Aruda M, Abdalla I, Singh A, Sweidan R, Gossinger H, Hirao K, Widman L, Jackman W. Radiofrequency catheter ablation of common type atrial flutter. *PACE.* 1993;16:850. Abstract.
26. Tanoi T, Komatsu C, Ishinaga T, Tokuhisa Y, Makino H, Nomoto J, Mogi J, Okamura T. Study on the genesis of the double potential recorded in the high right atrium in atrial flutter and its role in the reentry circuit of atrial flutter. *Am Heart J.* 1991;121:57-61.[\[Medline\]](#) [\[Order article via Infotrieve\]](#)
27. Feld GK, Shahandeh-Rad F. Mechanism of double potentials recorded during sustained atrial flutter in the canine right atrial crush injury model. *Circulation.* 1992;86:628-641.[\[Abstract/Free Full Text\]](#)
28. Yamashita T, Inoue H, Nozaki A, Sugimoto T. Role of anatomic architecture in sustained atrial reentry and double potentials. *Am Heart J.* 1992;124:938-946.[\[Medline\]](#) [\[Order article via Infotrieve\]](#)
29. Shimizu A, Nozaki A, Rudy Y, Waldo AL. Characterization of double potentials in a functionally determined reentrant circuit: multiplexing studies during interruption of atrial flutter in the canine pericarditis model. *J Am Coll Cardiol.* 1993;22:2022-2032.[\[Abstract\]](#)
30. Waldo AL, Plumb VJ, Arciniegas JG, MacLean W, Cooper TB, Priest MF, James TN. Transient entrainment and interruption of atrioventricular bypass pathway type of paroxysmal atrial tachycardia: a model for understanding and identifying reentrant arrhythmias. *Circulation.* 1983;67:73-83.[\[Free Full Text\]](#)
31. Stevenson WG, Woo MA. Determinants of antidromic wavefront propagation during entrainment of reentrant arrhythmias. *J Cardiovasc Electrophysiol.* 1991;2:215-223.
32. Fontaine G, Frank R, Tonet J, Grosgeat Y. Identification of a zone of slow conduction appropriate for ventricular tachycardia ablation: theoretical considerations. *PACE.* 1989;11:775-782.
33. Morady F, Kadish A, Rosenheck S, Calkins H, Kou WH, de Buitler M, Sousa J. Concealed entrainment as a guide for catheter ablation of ventricular tachycardia in patients with prior myocardial infarction. *J Am Coll Cardiol.* 1991;17:678-689.[\[Abstract\]](#)
34. Stevenson WG, Khan H, Sager P, Saxon LA, Middlekauff HR, Natterson PD, Wiener I. Identification of reentry circuit sites during catheter mapping and radiofrequency ablation of ventricular tachycardia late after myocardial infarction. *Circulation.* 1993;88:1647-1670.[\[Abstract/Free Full Text\]](#)

35. Strickberger SA, Ravi S, Daoud EG, Niebauer MJ, Man KC, Morady F. The relationship between impedance and temperature during radiofrequency ablation of accessory pathways. *J Am Coll Cardiol*. 1995;25:294. Abstract.
36. Olgin JE, Kalman JM, Fitzpatrick AP, Lesh MD. Role of right atrial endocardial structures as barriers to conduction during human type I atrial flutter: activation and entrainment mapping guided by intracardiac echocardiography. *Circulation*. 1995;92:1839-1848.[[Abstract/Free Full Text](#)]
37. Boineau JP, Schuessler RB, Cain ME, Corr PB, Cox JL. Activation mapping during normal atrial rhythm and atrial flutter. In: Zipes DP, Jalife J, eds. *Cardiac Electrophysiology: From Cell to Bedside*. Philadelphia, Pa: WB Saunders Co; 1990:537-548.
38. Tabuchi T, Okumura K, Matsunaga T, Tsunoda R, Jougasaki M, Yasue H. Linear ablation of the isthmus between the inferior vena cava and the tricuspid annulus for the treatment of atrial flutter: a study in the canine atrial flutter model. *Circulation*. 1995;92:1312-1319.[[Abstract/Free Full Text](#)]
39. Poty H, Saoudi N, Anselme F, Letac B. Success of radiofrequency ablation of type I atrial flutter may be predicted using electrophysiological criteria. *PACE*. 1995;18:856. Abstract.
40. Fischer B, Haissaguerre M, Cauchemez B, Garrigues S, Gencel L, Poquet F, Clementy J. Frequency of recurrent atrial fibrillation after successful radiofrequency catheter ablation of common atrial flutter: results in 100 consecutive patients. *PACE*. 1995;18:856. Abstract.

Articles citing this article

A simple pacing method to diagnose postero-anterior (clockwise) cavo-tricuspid isthmus block after radiofrequency ablation

Europace. 2010;12:1290-1295,

[Abstract](#) | [Full Text](#) | [PDF](#)

Typical Atrial Flutter as a Risk Factor for the Development of Atrial Fibrillation in Patients Without Otherwise Demonstrable Atrial Tachyarrhythmias

Mayo Clin Proc.. 2008;83:646-650,

[Abstract](#) | [Full Text](#) | [PDF](#)

Right Atrial Cavotricuspid Isthmus: Anatomic Characterization with Multi-Detector Row CT

Radiology. 2008;247:658-668,

[Abstract](#) | [Full Text](#) | [PDF](#)

Right Isthmus Ablation Reduces Supraventricular Arrhythmias After Surgery for Chronic Atrial Fibrillation

Ann. Thorac. Surg.. 2008;85:39-48,

[Abstract](#) | [Full Text](#) | [PDF](#)

Cardiac Conduction System: Anatomic Landmarks Relevant to Interventional Electrophysiologic Techniques Demonstrated with 64-Detector CT

RadioGraphics. 2007;27:1539-1565,

[Abstract](#) | [Full Text](#) | [PDF](#)

Platelet activation and myocardial necrosis in patients undergoing radiofrequency and cryoablation of isthmus-dependent atrial flutter

Europace. 2007;9:490-495,

[Abstract](#) | [Full Text](#) | [PDF](#)

Is inducibility of atrial fibrillation after radio frequency ablation really a relevant prognostic factor?

Eur Heart J. 2006;27:2553-2559,

[Abstract](#) | [Full Text](#) | [PDF](#)

Current strategies in the management of atrial fibrillation.

Ann. Thorac. Surg.. 2006;82:357-364,

[Abstract](#) | [Full Text](#) | [PDF](#)

Prospective randomised comparison of irrigated-tip and large-tip catheter ablation of cavotricuspid isthmus-dependent atrial flutter

Eur Heart J. 2004;25:963-969,

[Abstract](#) | [Full Text](#) | [PDF](#)

Left Septal Atrial Flutter: Electrophysiology, Anatomy, and Results of Ablation

Circulation. 2004;109:2440-2447,

[Abstract](#) | [Full Text](#) | [PDF](#)

Catheter-Based Cryoablation Permanently Cures Patients With Common Atrial Flutter

Circulation. 2004;109:1636-1639,

[Abstract](#) | [Full Text](#) | [PDF](#)

Typical atrial flutter ablation outcome: correlation with isthmus anatomy using intracardiac echo 3D reconstruction

Europace. 2004;6:407-417,

[Abstract](#) | [Full Text](#) | [PDF](#)

Atrial fibrillation II: rationale for surgical treatment

J. Thorac. Cardiovasc. Surg.. 2003;126:1693-1699,

[Full Text](#) | [PDF](#)

Acute and long-term results of radiofrequency ablation of common atrial flutter and the influence of the right atrial isthmus ablation on the occurrence of atrial fibrillation

Eur Heart J. 2003;24:956-962,

[Abstract](#) | [Full Text](#) | [PDF](#)

Characterization of Left Atrial Activation in the Intact Human Heart

Circulation. 2003;107:733-739,

[Abstract](#) | [Full Text](#) | [PDF](#)

Noninvasive, direct visualization of macro-reentrant circuits by using magnetocardiograms: initiation and persistence of atrial flutter

Europace. 2003;5:343-350,

[Abstract](#) | [Full Text](#) | [PDF](#)

Surgical treatment of atrial fibrillation: a review

Europace. 2003;5:S20-S29,

[Abstract](#) | [Full Text](#) | [PDF](#)

Sensitivity and specificity of concealed entrainment for the identification of a critical isthmus in the atrium: relationship to rate, anatomic location and antidromic penetration

J Am Coll Cardiol. 2002;39:896-906,

[Abstract](#) | [Full Text](#) | [PDF](#)

Cardioplegic arrest with L-arginine improves myocardial protection: results of a prospective randomized clinical trial

Ann. Thorac. Surg.. 2002;73:837-841,

[Abstract](#) | [Full Text](#) | [PDF](#)

Atypical atrial flutter: clinical features, electrophysiological characteristics and response to radiofrequency catheter ablation

Europace. 2002;4:241-253,

[Abstract](#) | [PDF](#)

Primary closed cooled tip ablation of typical atrial flutter in comparison to conventional radiofrequency ablation

Europace. 2002;4:265-271,

[Abstract](#) | [PDF](#)

Acute resumption of conduction in the cavotricuspid isthmus after catheter ablation in patients with common atrial flutter: Real-time evaluation and long-term follow-up

Europace. 2002;4:255-263,

[Abstract](#) | [PDF](#)

The use of advanced mapping systems to guide right linear lesions in paroxysmal atrial fibrillation

Eur Heart J Suppl. 2001;3:P41-P46,

[Abstract](#) | [PDF](#)

Double potentials along the ablation line as a guide to radiofrequency ablation of typical atrial flutter

J Am Coll Cardiol. 2001;38:750-755,

[Abstract](#) | [Full Text](#) | [PDF](#)

A classification of atrial flutter and regular atrial tachycardia according to electrophysiological mechanisms and anatomical bases. A Statement from a Joint Expert Group from the Working Group of Arrhythmias of the European Society of Cardiology and the North American Society of Pacing and Electrophysiology

Eur Heart J. 2001;22:1162-1182,
[PDF](#)

Atypical Right Atrial Flutter Patterns

Circulation. 2001;103:3092-3098,
[Abstract](#) | [Full Text](#) | [PDF](#)

Electromagnetic Versus Fluoroscopic Mapping of the Inferior Isthmus for Ablation of Typical Atrial Flutter : A Prospective Randomized Study

Circulation. 2000;102:2082-2086,
[Abstract](#) | [Full Text](#) | [PDF](#)

Differential Pacing for Distinguishing Block From Persistent Conduction Through an Ablation Line

Circulation. 2000;102:1517-1522,
[Abstract](#) | [Full Text](#) | [PDF](#)

Importance of Atrial Flutter Isthmus in Postoperative Intra-Atrial Reentrant Tachycardia

Circulation. 2000;102:1283-1289,
[Abstract](#) | [Full Text](#) | [PDF](#)

ELECTROPHYSIOLOGY: Treatment of atrial flutter

Heart. 2000;84:227,
[Full Text](#) | [PDF](#)

Multisite pacing for prevention of atrial tachyarrhythmias: potential mechanisms

J Am Coll Cardiol. 2000;35:1939-1946,
[Abstract](#) | [Full Text](#) | [PDF](#)

Right Atrial Angiographic Evaluation of the Posterior Isthmus : Relevance for Ablation of Typical Atrial Flutter

Circulation. 2000;101:2178-2184,
[Abstract](#) | [Full Text](#) | [PDF](#)

Global Right Atrial Mapping of Human Atrial Flutter: The Presence of Posteromedial (Sinus Venosa Region) Functional Block and Double Potentials : A Study in Biplane Fluoroscopy and Intracardiac Echocardiography

Circulation. 2000;101:1568-1577,
[Abstract](#) | [Full Text](#) | [PDF](#)

Catheter ablation of atrial flutter due to amiodarone therapy for paroxysmal atrial fibrillation

Eur Heart J. 2000;21:565-572,
[Abstract](#) | [PDF](#)

Prospective Randomized Comparison of Irrigated-Tip Versus Conventional-Tip Catheters for Ablation of Common Flutter

Circulation. 2000;101:772-776,
[Abstract](#) | [Full Text](#) | [PDF](#)

Effects of Tetrahydrobiopterin on Endothelial Dysfunction in Rats with Ischemic Acute Renal Failure

J. Am. Soc. Nephrol.. 2000;11:301-309,
[Abstract](#) | [Full Text](#) | [PDF](#)

A jump in cycle length of orthodromic common atrial flutter during catheter ablation at the isthmus between the inferior vena cava and tricuspid annulus: Evidence of dual isthmus conduction directed to dual septal exits

Europace. 2000;2:163-171,
[Abstract](#) | [PDF](#)

Cavotricuspid Isthmus Mapping to Assess Bidirectional Block During Common Atrial Flutter Radiofrequency Ablation

Circulation. 1999;100:2507-2513,
[Abstract](#) | [Full Text](#) | [PDF](#)

Modification of the Substrate for Maintenance of Idiopathic Human Atrial Fibrillation : Efficacy of Radiofrequency Ablation Using Nonfluoroscopic Catheter Guidance

Circulation. 1999;100:2085-2092,
[Abstract](#) | [Full Text](#) | [PDF](#)

Transverse conduction capabilities of the crista terminalis in patients with atrial flutter and atrial fibrillation

J Am Coll Cardiol. 1999;34:363-373,

[Abstract](#) | [Full Text](#) | [PDF](#)

Angiographic Anatomy of the Inferior Right Atrial Isthmus in Patients With and Without History of Common Atrial Flutter

Circulation. 1999;99:3017-3023,

[Abstract](#) | [Full Text](#) | [PDF](#)

Partial cavotricuspid isthmus block before ablation in patients with typical atrial flutter

J Am Coll Cardiol. 1999;33:1996-2002,

[Abstract](#) | [Full Text](#) | [PDF](#)

Rate-Dependent Conduction Block of the Crista Terminalis in Patients With Typical Atrial Flutter : Influence on Evaluation of Cavotricuspid Isthmus Conduction Block

Circulation. 1999;99:2771-2778,

[Abstract](#) | [Full Text](#) | [PDF](#)

Right Atrial Flutter Due to Lower Loop Reentry : Mechanism and Anatomic Substrates

Circulation. 1999;99:1700-1705,

[Abstract](#) | [Full Text](#) | [PDF](#)

Sodium nitroprusside during coronary artery bypass grafting: evidence for an antiinflammatory action

Ann. Thorac. Surg.. 1999;67:1059-1064,

[Abstract](#) | [Full Text](#) | [PDF](#)

LocaLisa : New Technique for Real-Time 3-Dimensional Localization of Regular Intracardiac Electrodes

Circulation. 1999;99:1312-1317,

[Abstract](#) | [Full Text](#) | [PDF](#)

Radiofrequency Catheter Ablation of Common Atrial Flutter : Significance of Palpitations and Quality-of-Life Evaluation in Patients With Proven Isthmus Block

Circulation. 1999;99:534-540,

[Abstract](#) | [Full Text](#) | [PDF](#)

High-Density Mapping of Activation Through an Incomplete Isthmus Ablation Line

Circulation. 1999;99:211-215,

[Abstract](#) | [Full Text](#) | [PDF](#)

Electrophysiological determinant for induction of isthmus dependent counterclockwise and clockwise atrial flutter in humans

Heart. 1999;81:73-81,

[Abstract](#) | [Full Text](#)

Successful Irrigated-Tip Catheter Ablation of Atrial Flutter Resistant to Conventional Radiofrequency Ablation

Circulation. 1998;98:835-838,

[Abstract](#) | [Full Text](#) | [PDF](#)

Atrial Fibrillation After Radiofrequency Ablation of Type I Atrial Flutter : Time to Onset, Determinants, and Clinical Course

Circulation. 1998;98:315-322,

[Abstract](#) | [Full Text](#) | [PDF](#)

Can L-arginine improve myocardial protection during cardioplegic arrest? Results of a phase I pilot study

Ann. Thorac. Surg.. 1998;66:108-112,

[Abstract](#) | [Full Text](#) | [PDF](#)

Three-dimensional Mapping of the Common Atrial Flutter Circuit in the Right Atrium

Circulation. 1997;96:3904-3912,

[Abstract](#) | [Full Text](#)

Relationship Between Atrial Fibrillation and Typical Atrial Flutter in Humans : Activation Sequence Changes During Spontaneous Conversion

Circulation. 1997;96:3484-3491,

[Abstract](#) | [Full Text](#)

Characterization of Low Right Atrial Isthmus as the Slow Conduction Zone and Pharmacological Target in Typical Atrial Flutter

Circulation. 1997;96:2601-2611.